Energy Conversion and Management 86 (2014) 735–744

Contents lists available at ScienceDirect

Energy Conversion and Management

journal homepage: www.elsevier.com/locate/enconman

Optimization of catalytic glycerol steam reforming to light olefins using Cu/ZSM-5 catalyst

Z.Y. Zakaria [a], N.A.S. Amin [a,*], J. Linnekoski [b]

[a] Chemical Reaction Engineering Group, Faculty of Chemical Engineering, Universiti Teknologi Malaysia, 81310 UTM Skudai, Malaysia
[b] VTT, Process Chemistry, Biologinkuja 7, P.O. Box 1000, FI-02044 VTT, Finland

ARTICLE INFO

Article history:
Received 3 October 2013
Accepted 15 June 2014

Keywords:
Glycerol to olefin
Catalytic conversion
Process optimization

ABSTRACT

Response surface methodology (RSM) and multi-objective genetic algorithm was employed to optimize the process parameters for catalytic conversion of glycerol, a byproduct from biodiesel production, to light olefins using Cu/ZSM-5 catalyst. The effects of operating temperature, weight hourly space velocity (WHSV) and glycerol concentration on light olefins selectivity and yield were observed. Experimental results revealed the data adequately fitted into a second-order polynomial model. The linear temperature and quadratic WHSV terms gave significant effect on both responses. Optimization of both the responses indicated that temperature favouring high light olefin formation lied beyond the experimental design range. The trend in the temperature profile concurred commensurately with the thermodynamic analysis. Multi-objective genetic algorithm was performed to attain a single set of processing parameters that could produce both the highest light olefin selectivity and yield. The turn-over-frequency (TOF) of the optimized responses demonstrated a slightly higher value than the one which was not optimized. Combination of RSM, multi-objective response and thermodynamic is useful to determine the process optimal operating conditions for industrial applications.

1. Introduction

Biodiesel is an alternative bioenergy produced from renewable resources such as palm, canola, soya bean and rape seed oil [1]. It can be produced via transesterification reaction of fatty acids and alcohols. Approximately 10 wt.% of glycerol, an alcohol with three hydroxyl groups is produced as a byproduct in this reaction [2–4]. The crude glycerol obtained is 50% pure with huge potential as a raw material to produce valuable products [5] including gas phase [6]. With more crude glycerol being generated from biodiesel production as a by-product, continuous efforts are inherently seeked to manage and convert glycerol to useful chemicals economically which can indirectly minimize the cost of biodiesel production.

Glycerol can be converted to various precious products such as fuel additives [7], acrolein [5,8–10], propane [11] 1-hydroxyacetone [12], formaldehyde [5], acetol [5], alkyl aromatics [13], and hydrogen [14,15]. In several reports involving glycerol dehydration [8,11,16–18], light olefins have been detected as side product of the reaction. Corma [8] obtained some light olefins while catalytically testing glycerol to acrolein with zeolite ZSM-5. In a separate study, Murata and co-workers found propylene when testing glycerol to propane using ZSM-5 zeolite catalyst [11]. Recently, Zakaria [19] compared several metal-loaded ZSM-5 catalysts to convert glycerol to light olefin with Cu/ZSM-5 exhibited the best performance. It is worthy to note that dedicated research on glycerol conversion to olefin is relatively new and very much at its infancy stage.

The impact for light olefins research is huge since the chemicals have such high commercial value and industrial importance. Literatures concerning glycerol transformation to light olefins are limited. However, studies involving methanol and ethanol to light olefins over zeolite catalysts [20–23] are abundant inferring that glycerol, being in the same alcohol group as methanol and ethanol, has the potential to be converted to light olefins. In another development, the utilization of biomass such as rice husk, sawdust and sugarcane bagasse to produce light olefin has also progressively gain attention [24].

Olefin is basically a petrochemical derivative conventionally produced by thermal cracking of natural gas and crude oil in refineries worldwide. Ethylene is the simplest olefin with only two carbon atoms. Major olefin products like ethylene, propylene, butadiene and C_4 derivatives, better known as light olefins are used to produce plastics, chemical intermediates, and industrial solvents [25]. The exorbitant price of light olefin can be reduced [26] by utilizing glycerol, as a feed, and establishing a commercially and economically viable process. In addition, the

* Corresponding author. Tel.: +60 7 5535553; fax: +60 7 55881463.
E-mail address: noraishah@cheme.utm.my (N.A.S. Amin).

http://dx.doi.org/10.1016/j.enconman.2014.06.040
0196-8904/

overall process is environmentally friendly since the feed stock to produce light olefin is from a renewable source.

The main objective of this paper is to determine the optimal process parameters for conversion of glycerol to light olefins using response surface methodology (RSM). The RSM technique attempts to optimize light olefin selectivity and yield individually at the corresponding process parameters. A central composite rotatable design is used for design of experiment. The empirical mathematical models for olefin selectivity and yield are also generated. The statistical analysis is also implemented to testify the adequacy of the models. Imperatively, multi-objective genetic algorithm is employed to determine the maximum light olefin selectivity and yield simultaneously at the corresponding optimal independent variables. The turn-over-frequency (TOF) of the catalyst at the optimized process is also evaluated. The RSM, multi-objective genetic algorithm and TOF analysis for the conversion of glycerol to light olefin have not been presented and discussed previously by other researchers. In order to provide better comprehension of the optimum operating condition results, the discussion is correlated with thermodynamic analysis for ethylene, which represents light olefins. Finally, a view on the available technologies and the cost of corresponding feedstock to produce light olefin is presented, providing insight on the economic cost conjecture.

2. Materials and method

2.1. Materials

The main reagents were HZSM-5 (SiO_2/nAl_2O_3 = 30; Zeolyst, USA), and glycerol (87.5% purity; Merck, USA). Copper nitrate from Emory Laboratory Reagents was used to impregnate HZSM-5.

2.2. Catalyst preparation

Cu/ZSM-5 catalyst was prepared according to the wet-impregnation method. Initially, the parent HZSM-5 zeolite was added into 100 ml of distilled water before 30 wt% of copper nitrate salt was added into the solution, mixed and stirred at 60–70 °C temperature for an hour. The solution was then dried at 100 °C for 12 h and finally calcined at 550 °C for 5 h. The calcined catalyst was then crushed and sieved between 40 and 50 mesh to obtain uniform catalyst size for the catalytic cracking of glycerol with steam.

2.3. Catalyst characterization

Cu/ZSM-5 was characterized by XRD, FTIR, BET, TPD-ammonia and TPR. It has comparatively larger surface area and higher acidity than other metal ZSM-5 studied earlier [19]. Detail characterization methods as well as chemical and physical properties of Cu/ZSM-5 have been discussed elsewhere [19]. The characterization results reveal that the physico-chemical properties of Cu/ZSM-5 is suitable for the catalytic conversion of glycerol to olefins, as significantly shown from the higher distribution of strong acid sites.

2.4. Catalytic performance test

Catalyst testing was performed in a fixed-bed quartz reactor, with outside diameter = 13 mm and length = 35 cm, positioned inside a vertical *Carbolite* tubular furnace. Prior to testing, the catalyst was activated in helium gas flow for 1 h at 500 °C. After the catalyst has been reduced, glycerol solution was vaporized and fed at temperature between 300 and 310 °C. A set of thermocouples attached to a temperature data logger was fixed along the line to monitor the temperature reading at various locations. The purpose was mainly to ensure that glycerol did not condense before entering the reactor. The processing parameters were temperatures 511.8–688.2 °C, WHSV 25.6–184.4 h^{-1} and glycerol concentration of 12.4–47.6% at atmospheric pressure. The gaseous products were then analyzed with an on-line HP 6890N GC-TCD/FID gas chromatography equipped with both thermal conductive detector (TCD) and flame ionization detector (FID). The columns used were HP plot/Q, HP-Mole sieve, GP-Gaspro and Hayasep-Q for the main product analysis. The final amount of gaseous products as well as liquid was recorded for the overall mass balance calculation to provide the amount of coke. The liquid was analyzed to determine unreacted glycerol for glycerol conversion calculation. A detail liquid analysis was not performed in this study since light olefins production was the main focus. The schematic experimental set-up is shown in Fig. 1. The glycerol conversion, selectivity and yield of products are each defined by Eqs. (1)–(3):

$$\text{Glycerol conversion}\ (\%) = \frac{\text{Amount of glycerol converted (mol)}}{\text{Total amount of glycerol in the feed (mol)}} \times 100 \quad (1)$$

$$\text{Olefin selectivity}\ (\%),\ S = \frac{\text{Amount of olefins (mol)}}{\text{Amount of all products (mol)}} \times 100 \quad (2)$$

$$\text{Olefin yield}\ (\%,\ Y) = \frac{\text{Amount of olefins (mol)}}{\text{Amount of glycerol feed (mol)}} \times 100 \quad (3)$$

Only selectivity and yield of gaseous products, specifically light olefins, are discussed in this study in view of their commercial importance.

2.5. Experimental design

Investigating a five level three factor Central Composite Design (CCD) using Statistika version 7.0 required 16 experiments in this study. Eight star points ($\alpha = \pm 1$), six axial points ($\alpha = \pm 2$) and two replicates at the center point ($\alpha = 0$) were chosen as experimental points. Central points were used to check the reproducibility and stability of results. The runs were conducted in randomized manner to guard against systematic bias. The performance of the process was evaluated by analyzing the (1) selectivity and (2) yield as the responses. Each run was performed in duplicate.

For experimental design of the catalytic steam reforming of glycerol; temperature, WHSV and glycerol concentration were chosen as the parameters that would most likely influence the performance of the system. The low, middle and high levels of all the independent variables were based on prior screening of the literatures and designed for future economic pilot scale operation, as listed in Table 1.

The substitution of the chosen parameters into the resulting model enabled the calculation of the predicted response as shown in Eq. (4),

$$\eta = \beta_0 + \sum_{i=1}^{3}\beta_i x_i + \sum_{i=1}^{3}\beta_{ii}x_i^2 + \sum_{i=1}\sum_{j=i+1}^{3}\beta_{ii}x_i x_j + \varepsilon \quad (4)$$

where η is the response, β_0 is constant coefficient, β_i, β_{ii}, and β_{ij} are linear, quadratic and second order interaction coefficient, respectively. x_i and x_j are independent variables where e is the error. The *R-square* was determined by Eq. (5),

$$R^2 = 1 - \frac{SS_{\text{Residual}}}{SS_{\text{model}} + SS_{\text{Residual}}} \quad (5)$$

where SS is the sum of square and degree of freedom, respectively. *R-Square* is the most important factor in examining the variability of

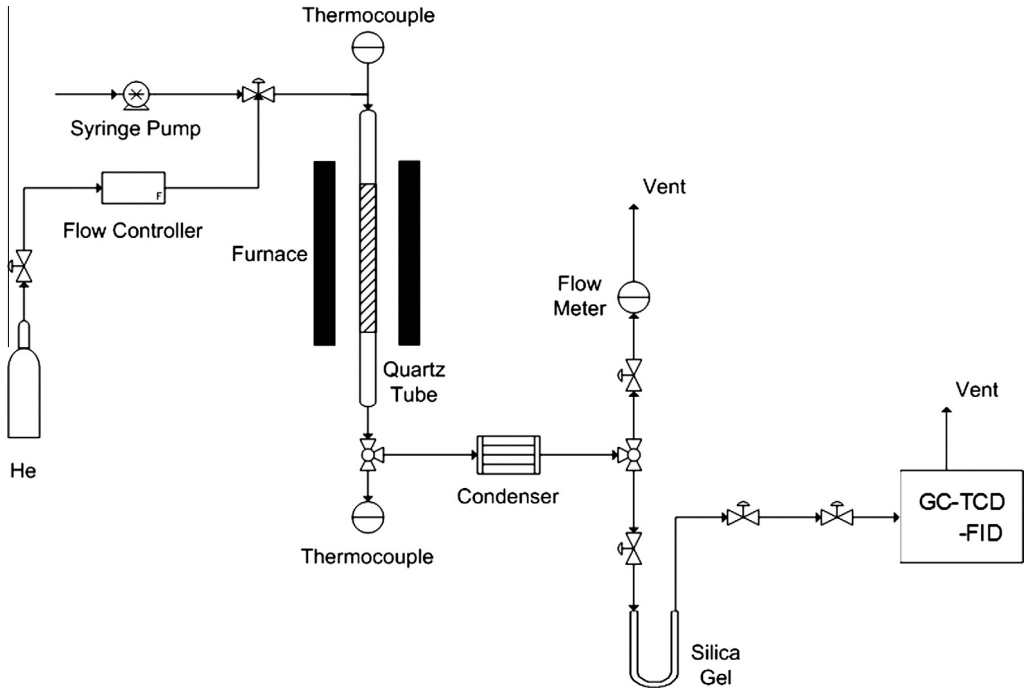

Fig. 1. Schematic experimental set up.

Table 1
Experimental level coded and range of independent parameters.

Independent process parameters		Coded levels of parameters				
		$-\alpha$	-1	0	+1	$+\alpha$
Temperature (°C)	X_1	511.8	550.0	600.0	650.0	688.2
WHSV (h^{-1})	X_2	25.6	60.0	105.0	150.0	184.4
Glycerol concentration (%)	X_3	12.4	20.0	30.0	40.0	47.6

independent variables. Meanwhile, the *F*-test is for checking the statistical significance of the model. The number of experiments, experimental conditions and results are summarized in Table 2.

3. Results and discussion

Glycerol was completely converted in all runs as no trace of glycerol was detected in the liquid product. Analysis on thermodynamic equilibrium for steam reforming of glycerol has also verified this [27,28]. Light olefin selectivity and yield are calculated according to Eqs. (2) and (3).

3.1. Single response optimization for light olefin selectivity and yield

The responses, olefin selectivity (S) and olefin yield (Y), are correlated with the three variables studied by using multiple regression analysis, employing a second order polynomial as presented by Eq. (4). Regression analysis was carried out using STATISTICA software, which was later also utilized to determine the significance of each factor investigated. A regression equation for S and Y as a function of temperature (X_1), WHSV (X_2) and glycerol concentration (X_3) and their interaction using linear and quadratic regression coefficient of main factors and linear-by-linear regression coefficients of interaction are derived, as presented in Eqs. (6) and (7):

Table 2
Central composite design of three independent parameters with experimental and RSM response values.

Run	Location	Coded values (actual values)			Response 1:% olefin selectivity		Response 2:% olefin yield	
		Temp. (°C)	WHSV (h^{-1})	Gly. Dil. (%)	Observed	RSM	Observed	RSM
1	Star	−1 (550.0)	−1 (60)	−1 (20)	19.4	19.5	14.8	14.9
2	Star	−1 (550.0)	−1 (60)	+1 (40)	20.9	20.7	15.3	15.3
3	Star	−1 (550.0)	+1 (150)	−1 (20)	20.1	19.9	13.9	14.1
4	Star	−1 (550.0)	+1 (150)	+1 (40)	21.3	20.6	15.1	15.0
5	Star	+1 (650.0)	−1 (60)	−1 (20)	20.8	21.2	15.9	16.5
6	Star	+1 (650.0)	−1 (60)	+1 (40)	21.9	21.9	16.1	16.5
7	Star	+1 (650.0)	+1 (150)	−1 (20)	21.9	21.8	15.7	16.2
8	Star	+1 (650.0)	+1 (150)	+1 (40)	22.4	22.0	16.4	16.7
9	Center	0 (600.0)	0 (105)	0 (30)	21.7	21.8	16.7	16.7
10	Axial	$-\alpha$ (511.8)	0 (105)	0 (30)	19.6	20.0	14.6	14.7
11	Axial	$+\alpha$ (688.2)	0 (105)	0 (30)	22.9	22.7	18.4	17.6
12	Axial	0 (600.0)	$-\alpha$ (25.6)	0 (30)	20.4	20.0	15.5	15.1
13	Axial	0 (600.0)	$+\alpha$ (184.4)	0 (30)	19.9	20.5	14.9	14.6
14	Axial	0 (600.0)	0 (105)	$-\alpha$ (12.4)	20.9	20.6	16.0	15.4
15	Axial	0 (600.0)	0 (105)	$+\alpha$ (47.6)	21.2	21.8	16.2	16.1
16	Center	0 (600.0)	0 (105)	0 (30)	21.9	21.8	16.9	16.7
R_2 values						0.8643		0.8802

$$S = 0.0001X_1^2 - 0.0002X_2^2 - 0.0020X_3^2 + 0.0916X_1 + 0.0459X_2 + 3.387X_3 + 0.0001X_1X_2 + 0.0003X_1X_3 + 0.0003X_2X_3 - 18.50 \quad (6)$$

$$Y = 0.0001X_1^2 - 0.0003X_2^2 - 0.2942X_3^2 + 0.1023X_1 + 0.0157X_2 + 0.2942X_3 + 0.0001X_1X_2 - 0.0002X_1X_3 + 0.0003X_2X_3 - 24.2426 \quad (7)$$

The coefficients with one factor represent the effect of the particular factor, while the coefficients with two factors signify interaction between the two terms. Coefficients with second order terms denote the quadratic effect of the factor. The positive and negative signs in front of each coded variables indicate parallel and adverse effect of the factors to the responses respectively. The models were selected based on the highest order of polynomials where the models were significant and not aliased.

The main effects model indicated that the quadratic term for glycerol concentration has the highest negative effect on light olefin selectivity as observed through beta regression coefficient, whereas, glycerol concentration linear term has highest positive effect on light olefin selectivity. On the other hand, the interaction between temperature and glycerol concentration as well as the quadratic term for WHSV and glycerol concentration showed negative effect toward light olefin yield. The linear temperature term has the highest positive contribution as observed from the regression term compared to others for light olefin yield. Generally, it is evident that all interaction terms showed positive effect for both responses except for the interaction between temperature and glycerol concentration for light olefin yield.

Having generated the regression model equation to represent the effect of each variable including their interactions with each other on the S and Y values, analysis to evaluate the adequacy of the model was performed. The first criteria evaluated to determine the model adequacy is by judging the appropriateness of the model from the determination coefficient, the R-squared value, which reveals the total variation of the observed values of activity about its mean [29].

The R^2 for the regression model relating all three effects are 0.86428 and 0.88024 for S and Y, respectively, which is considered good in describing the validity of the models generated. According to the R^2 for S, 86.4% of the sample variation could be attributed to the variable and only 13.6% of the total variance could not be explained by the models. Similarly for Y, 88.0% of the samples are ascribed by the measured variable and 12.0% are not. Using the regression model generated, a predicted value for the response in each run according to the experimental design was obtained, as listed in Table 2.

Fig. 2 depicts the variation of the experimental data against the predicted value for both S and Y. From Fig. 2(a), it could clearly be observed that the linear red line plotted using points calculated according to the regression model deviates very slightly from S_{exp} where $S_{exp} = S_p$, and S_{exp} and S_p are selectivity from experimental and predicted data, respectively, showing appropriateness of the model generated. The predicted values calculated from the regression model also in majority falls very near to the line plotted as expected from the reasonably good value of R-squared. Fig. 2(b) shows similar scenario as depicted by Fig. 2(a). Generally, it can be stated that $Y_{exp} = Y_p$, where Y_{exp} and Y_p are yields from experimental and predicted Y, respectively, showing appropriateness of the model generated.

The adequacy of the generated regression models were also evaluated using ANOVA method, which is very useful to determine significant effects of process variables to the response and to fit the second order polynomial models to the experimental data [29].

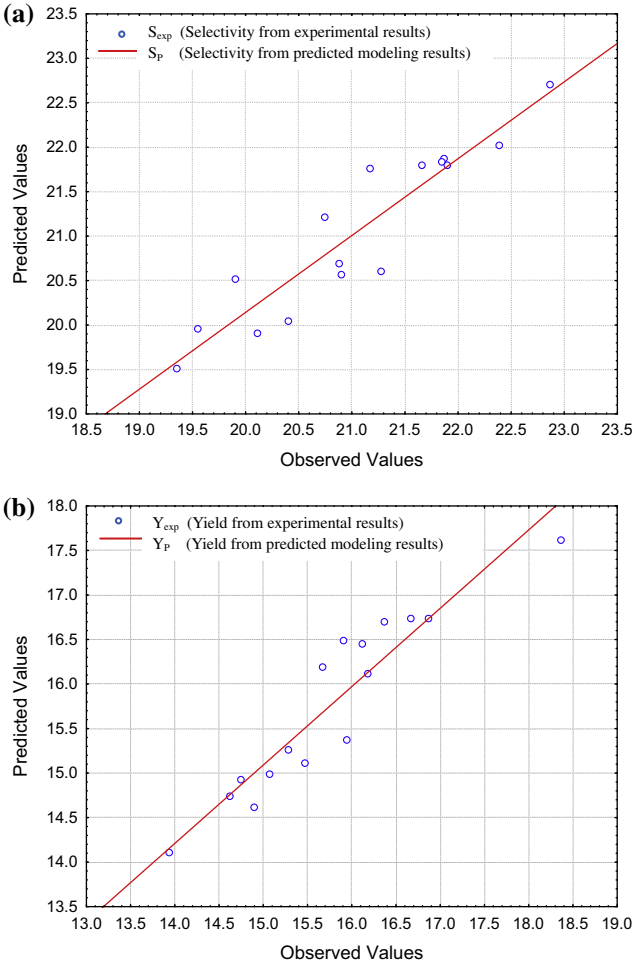

Fig. 2. Observed versus predicted value for (a) C_2H_4 Selectivity and (b) C_2H_4 Yield.

Table 3 lists the outcome of such analysis. In order to evaluate the adequacy or accuracy of the model using ANOVA, the important value to be observed is the F-value, which is the ratio of mean square due to regression to the mean square due to residual error. In general the F-value calculated from ANOVA should be greater than the tabulated value for the model to be considered appropriate. F-value calculated for the S model is 4.3, which exceeded the tabulated F-value for 95% confidence ($F_{0.05,9,6}$) (4.1) while the calculated F-value for Y is 4.9, which also exceeded the tabulated F value.

Once the validity and adequacy of the regression model has been assessed, it is very useful to identify the variables that would affect the process significantly. The factor with the lowest p-value and the highest F-value is considered the most significant. From Fig. 3(a), it is evident that the linear temperature term, X_1, has the most effect on S with p-value of 0.014918 at F-value 4.967. The next factor rated as significant is quadratic WHSV. The limiting value for p is 0.05, which is based on the confidence level fixed for the ANOVA analysis carried out; hence all factors with p-value lower than 5% are judged significant. Other factors not mentioned are all rated as insignificant to affect the value of S in the process. As for Y, the most significant factor is also the linear term of temperature, X_1, with p-value = 0.010454 and F-value = 5.3294, followed by the quadratic term of WHSV, as shown in Fig. 3(b). The p-values were obtained form the regression analysis tool in the software. This information concluded that both temperature and WHSV significantly affected the selectivity and yield, respectively.

Table 3
The results for ANOVA test for% olefin selectivity and% olefin yield.

	Sources	Sum of square	Degree of freedom	Mean square	*F* value	F tabulated
% Olefin selectivity	Regression	13.3547	9	1.483856	4.245446	4.1
	Residual	2.09710	6	0.349517		
	Total	15.45181	15			
% Olefin yield	Regression	14.7437	9	1.638185	4.90023	4.1
	Residual	2.00585	6	0.334308		
	Total	16.74951	15			

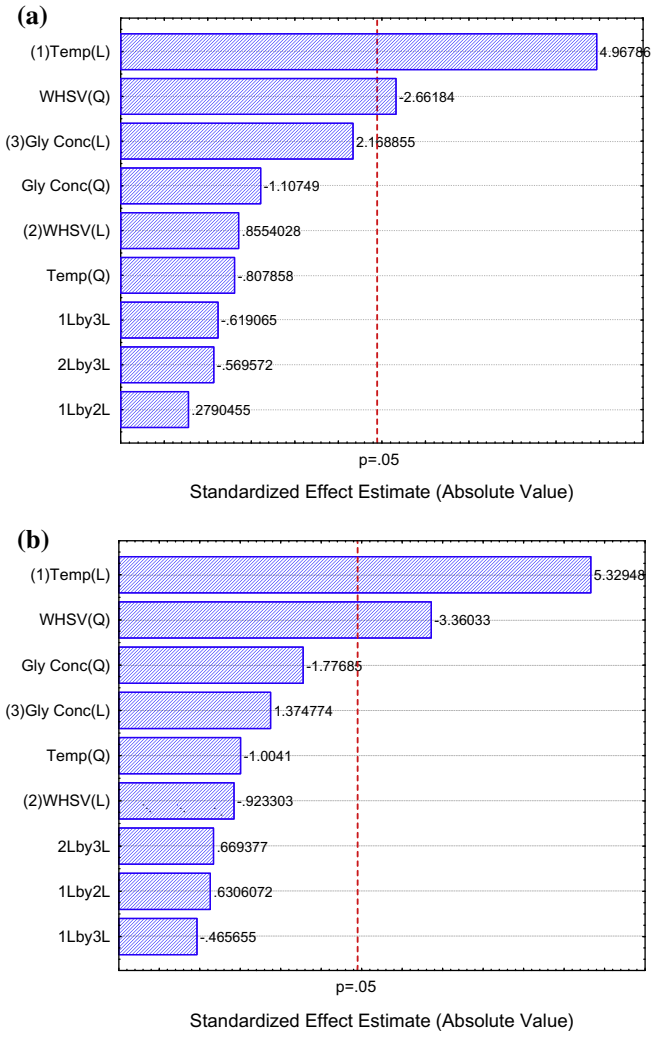

Fig. 3. Pareto Chart for (a) C_2H_4 selectivity and (b) C_2H_4 yield.

3.2. Response surface contour plots

Contour plots of the response toward variation of two factors at a time could be obtained to see their effect and interaction on the response at the center point of the other variable. Figs. 4 and 5 illustrates the contour plots for all possible combinations of two variables. The effects of any two independent variables on the response could be observed by plotting a 3D surface plot of the response against the other independent variables, as the third variable kept at the center of their range.

The contour plots presented in Fig. 4(a) for value of *S* as a function of temperature and WHSV with glycerol concentration kept at 30%, indicates that the selectivity, *S* increases with temperature. *S*

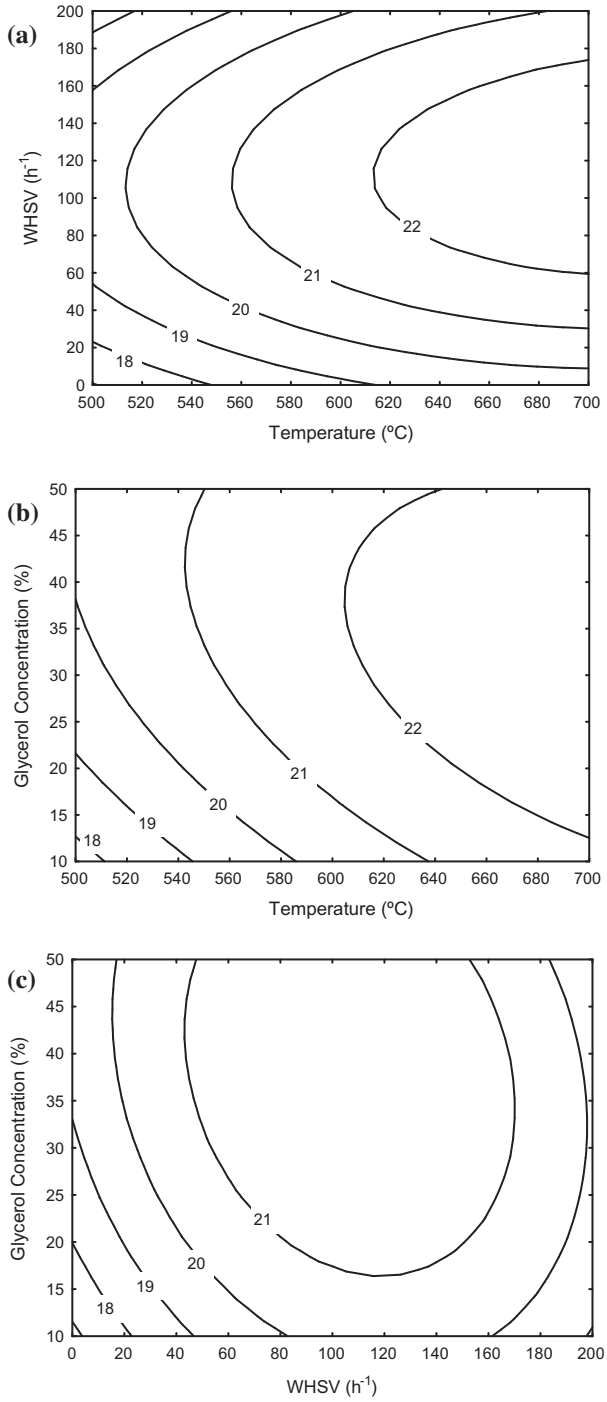

Fig. 4. Contour plots manifesting interactions between factors affecting *S* (a) graph of temperature versus WHSV for *S* when glycerol concentration is 30% (b) graph of temperature versus glycerol concentration for *S* when WHSV is 105 h^{-1} (c) graph of glycerol concentration versus WHSV for S when temperature is 600 °C.

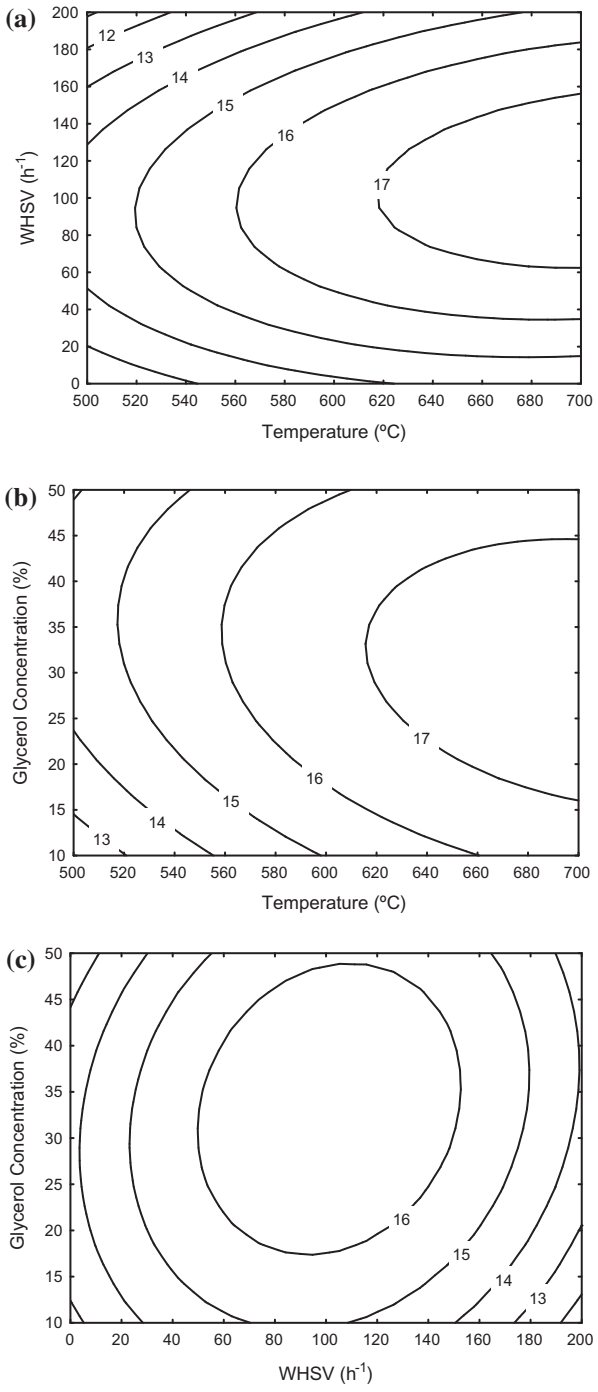

Fig. 5. Contour plots manifesting interactions between factors affecting *Y* (a) graph of temperature versus WHSV for *Y* when glycerol concentration is 30% (b) graph of temperature versus glycerol concentration for *Y* when WHSV is 105 h^{-1} (c) graph of glycerol concentration versus WHSV for *Y* when temperature is 600 °C.

also increases with WHSV, but decreases after 120 h^{-1}. The elliptical contour obtained portrays a perfect interaction between the independent variables [30]. It can be observed that the maximum *S* with respect to temperature lies beyond the parameter decided earlier in this study.

The surface temperature plot against glycerol concentration presented the interaction between both independent variables toward S while maintaining WHSV at 105^{-1}, in Fig. 4(b). It could be seen that *S* also increases and does not show sign of decreasing when temperature increases. This shows that the optimum temperature is situated beyond 700 °C. On the other hand, the effect of glycerol concentration toward S is identical to that explained earlier in Fig. 4(a). This demonstrated that the optimum glycerol concentration is between the 25% and 36% plateau.

The effects and interactions of glycerol concentration and WHSV were also investigated via a surface plot, presented in Fig. 4(c). As WHSV was increased, *S* increases. However, as the WHSV increased beyond 130 h^{-1}, *S* decreased. The plot reveals that the range of WHSV producing the highest possible *S* is between 70 and 130 h^{-1} at glycerol concentration between 24% and 42%.

Evident from Fig. 5(a), temperature and WHSV gave almost similar effects on *Y*; in concurrence to what was revealed for *S*. The effects and interactions of temperature and glycerol concentration on *Y* are illustrated in Fig. 5(b), while Fig. 5(c) depicts the effect and interaction of WHSV and glycerol concentration on the yield, *Y*. Both resemble almost the same pattern. For Fig. 5(a) and (b), the temperature exceeded the maximum range set for the design of experiment. It is probable the optimum temperature for both *S* and *Y* lied beyond 700 °C. Hence, it can be deduced that in general, the process parameters interaction in this study followed the same trend toward *S* and *Y*. It can be assumed that the formation of other gases, liquid, oxygenates and solid (coke), have negligible effect on *S* and *Y* for the light olefins.

3.3. Optimum operating conditions

The statistical software used is fully capable of generating a regression model to predict an appropriate value of the response, and also investigating the effect of each operating condition as well as their interaction with each other. The ultimate goal however, is to achieve or obtain a specific value for each variable involved in this investigation to finally determine the most efficient catalytic glycerol steam reforming process, provided by *S* and *Y* values. Table 4 tabulates the predicted results for *S* and *Y*. It can be seen that the values for WHSV and glycerol concentration are within the experimental range. However, the temperature value is high and beyond the maximum range. This implies that the light olefin selectivity and yield require higher temperature, more than the initial ceiling temperature value set in Table 1, which is 650 °C and even more than the alpha or extreme temperature value, 688 °C. Thermodynamic analysis of glycerol steam reforming illustrated in Fig. 6 reveals that ethylene production reached a maximum peak [31]. Generally, without catalyst, ethylene formation peaks between 600 and 800 °C depending on the glycerol to water (GWR) ratio [31]. Although the thermodynamic analysis gave good general indication of the optimum temperature range, the GWR 1:12 ratio employed in this study gave ethylene peak around 600 °C, which is the center value of temperature for RSM. It is however unfair to equate both conditions since the thermodynamic analysis was conducted without catalyst. However, the thermodynamic analysis reveals that if we compare the average

Table 4
Predicted responses for olefin selectivity (*S*) and yield (*Y*).

	% Olefin Selectivity				% Olefin Yield			
	Temp. (°C)	WHSV (h^{-1})	Glycerol conc. (%)	Optimum S	Temp. (°C)	WHSV (h^{-1})	Glycerol conc. (%)	Optimum Y
Predicted	737.80	119.36	28.7	22.9	715.88	110.95	30.1	17.7

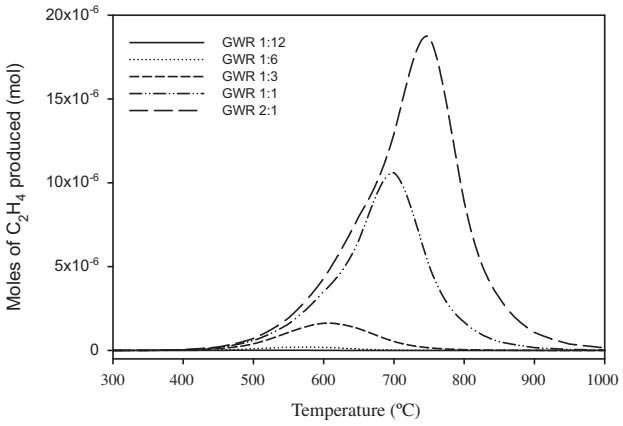

Fig. 6. Thermodynamic equilibrium of light olefin produced from glycerol.

of all GWR, the optimum temperature will be around 700 °C. Hence, the thermodynamic explanation supports the reason why the optimum temperature for both *S* and *Y* lied beyond 688 °C.

A total of 13 possible chemical reactions that could take place in glycerol steam reforming process are represented in equations R1–R13. Glycerol steam reforming (R1) and decomposition of glycerol (R2) are spontaneous reactions leading to a complete glycerol conversion. Series of reactions (R3–R7) which include hydrogenation took place before ethylene is formed via oxidative coupling of methane reactions (R8 and R9). Since the overall reaction is complex, ethylene, in this case, represents the total light olefin production. The inevitable coking process is represented by reactions R10–R13 where carbon (solid) is formed.

R1	Glycerol steam reforming	$C_3H_8O_{3(g)} + 3H_2O_{(g)} \leftrightarrow 3CO_{2(g)} + 7H_{2(g)}$	ΔH_{298} = 122.89 kJ/mol
R2	Decomposition of glycerol	$C_3H_8O_{3(g)} \leftrightarrow 4H_{2(g)} + 3CO_{(g)}$	ΔH_{298} = 246.31 kJ/mol
R3	Water gas shift reaction	$CO_{(g)} + H_2O_{(g)} \leftrightarrow H_{2(g)} + CO_{2(g)}$	ΔH_{298} = −41.14 kJ/mol
R4	Methanation	$CO_{(g)} + 3H_{2(g)} \leftrightarrow CH_{4(g)} + H_2O_{(g)}$	ΔH_{298} = −206.11 kJ/mol
R5	Methanation	$CO_{2(g)} + 4H_{2(g)} \leftrightarrow CH_{4(g)} + 2H_2O_{(g)}$	ΔH_{298} = −164.94 kJ/mol
R6	CO_2 reforming of methane	$CO_{2(g)} + CH_{4(g)} \leftrightarrow 2H_{2(g)} + 2CO_{(g)}$	ΔH_{298} = 247.28 kJ/mol
R7	Oxidative coupling of methane	$2CH_{4(g)} + CO_{2(g)} \leftrightarrow C_2H_{6(g)} + CO_{(g)} + H_2O_{(g)}$	ΔH_{298} = 106.00 kJ/mol
R8	Oxidative coupling of methane	$2CH_{4(g)} + 2CO_{2(g)} \leftrightarrow C_2H_{4(g)} + 2CO_{(g)} + 2H_2O_{(g)}$	ΔH_{298} = 284.00 kJ/mol
R9	Dehydrogenation of ethane	$C_2H_{6(g)} \leftrightarrow C_2H_{4(g)} + H_{2(g)}$	ΔH_{298} = 136.33 kJ/mol
R10	Methane decomposition	$CH_{4(g)} \leftrightarrow 2H_{2(g)} + C_{(s)}$	ΔH_{298} = 74.52 kJ/mol
R11	Disproportionation	$2CO_{(g)} \leftrightarrow CO_{2(g)} + C_{(s)}$	ΔH_{298} = −172.44 kJ/mol
R12	Hydrogenation of CO_2	$CO_{2(g)} + 2H_{2(g)} \leftrightarrow 2H_2O_{(g)} + C_{(s)}$	ΔH_{298} = −90.16 kJ/mol
R13	Hydrogenation of CO	$H_{2(g)} + CO_{(g)} \leftrightarrow H_2O_{(g)} + C_{(s)}$	ΔH_{298} = −131.3 kJ/mol

3.4. Multi-objective genetic algorithm optimization

The previous section utilizes design of experiment and only provides operating condition for a single response. When there are more than two responses, the optimum operating conditions will provide two or more sets. In order to optimize a process having two or more responses, a single set of operating parameter that is capable to optimize two or more responses is required. For this purpose, multi-objective genetic algorithm optimization using MATLAB was carried out. The multi-objective optimization provides a set of independent variables that maximizes two or more responses simultaneously, in this case to optimize *S* and *Y* concurrently. Prior to the optimization part, the experimental data was used for training of the network, where Levenberg–Marquardt algorithm was applied [32]. The minimum and maximum boundary was assigned to follow the initial processing parameters (as in Table 1) in the MATLAB *optimization tool* interface. After obtaining the best network, the genetic algorithm tool (gatool) available in MATLAB was launched, and the solver option for multi-objective optimization was selected (gamultiobj). At the end of the run, MATLAB produced several optimal conditions for optimum responses of *S* and *Y*. This then lead to the Pareto-optimal solutions for simultaneous optimization corresponding to *S* and *Y* as illustrated in Fig. 7. The choice of the final solution (optimal point) was based on the combination of *S* and *Y* producing the highest value. From there, a solution on the Pareto front that fulfilled this requirement was identified, as presented in Table 5.

As explained earlier, the result produced only a single optimized set of process parameters to optimize both *S* and *Y*. As desired, simulation results provided temperature, WHSV and glycerol concentration are within the range. The temperature value simulated is the maximum temperature, 650 °C, due to the maximum or ceiling value set earlier which would not allow it to go beyond the range. From the confirmatory experiments, an average was taken and compared with the simulated results. The percentage differences between the simulated and experimental values are below 2%. It can be inferred that the multi-objective genetic algorithm optimization successfully provide a single set of process parameter for optimum *S* and *Y*. Fig. 7 illustrates the Pareto front obtained during the multi-objective genetic algorithm optimization to attain the best dependent and independent responses. From this finding, it can be concluded that the optimum *S* (22.1%) and *Y* (17.8%) can be attained at 650 °C, 116.54 h^{-1} and 26.9% glycerol concentration.

Table 6 compares non-optimized and optimized values for the dependant and independent responses. It can be observed that the optimized process parameters produced slighly better light olefin selectivity and yield. This information is crucial for the optimization of glycerol steam reforming to light olefins and provides how the process parameters should be set in order to optimize the reaction.

3.5. Turnover frequency

The turnover frequency (TOF) for the optimized Cu/ZSM-5 to attain light olefin components, namely ethylene, propylene and butylene taken between 5 and 15 min was compared with that of the non-optimized conducted earlier [19], as exemplified in Fig. 8. The TOF in this case is defined as equal to the rate of olefin molecule produced per second per surface area of the catalyst. As expected, the TOF of the optimized reaction is slightly higher than the non-optimized reaction. Although the difference seems to be

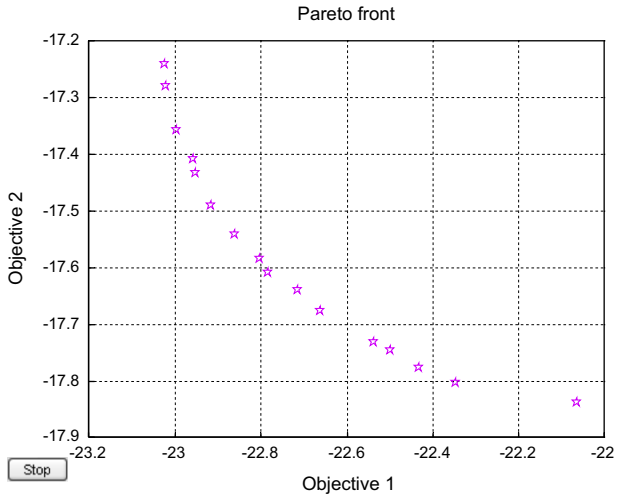

Fig. 7. Pareto front using genetic algorithm multiple objective.

small, such tiny improvement will significantly affect the overall production cost in a pilot or commercial scale process.

Since the chemical and physical properties of Cu/ZSM-5 were more favorable for light olefins formation compared to other catalysts screened earlier [19], the optimized condition is however, not related to the catalytic properties. The temperature program desorption ammonia (TPD-NH_3) and temperature program reduction (TPR) do not show any effect when temperature is increased from 500 to 700 °C. This indicates that the combination effect of the process parameters (temperature, WHSV and glycerol concentration) gives optimum performance over the Cu/ZSM-5 catalyst.

The TOF for optimum and non-optimum conditions have almost similar distribution of ethylene, propylene and butylene, with ethylene as the major component. The TOF for propylene for all catalysts were below 1 mol m^{-2} s^{-1} while for butylene, it is almost negligible. The TOF of CuZSM-5 for optimized condition increases when temperature is increased to 650 °C. Operating the process at about 600 °C will also yield light olefin but not as optimum as at 650 °C. This can be related to the light olefins thermodynamic equilibrium profile. Consequently, it is expected that the TOF of optimized Cu/ZSM-5 will decrease when tested beyond 700 °C.

At optimum WHSV, a higher TOF compared to the non-optimized one was observed. This is true since more glycerol vapor was adsorped onto the catalyst surface and reacted via dehydration, dehydrogenation and deoxygenation to produce lighter compounds. However, since the surface and micropore area of Cu/ZSM-5 is limited, it could not accommodate more glycerol vapor (with 30% concentration) above 116.54 h^{-1}. Performing the experiment at WHSV = 105 h^{-1} has proven that the amount of glycerol vapor is insufficient to fully utilize the surface and micropore area available for Cu/ZSM-5. Unfortunately, beyond 116.54 h^{-1}, the formation of light olefin decreased. This is mainly due to the fact that the light olefins competes heavily with the formation toward hydrogen and CO. It is tough to explain the reason why glycerol with concentration lower than the non-optimized produced more light olefins. Ideally, higher glycerol concentration,

Table 6
Comparison between non-optimized and optimized dependent and independent responses using multi-objective genetic algorithm optimization.

	Non-optimized	Optimized
Temperature (°C)	600.00	650.00
WHSV (h^{-1})	105.00	116.54
Glycerol concentration (%)	30.00	26.91
Selectivity (%)	20.2	22.1
Yield (%)	16.3	17.8

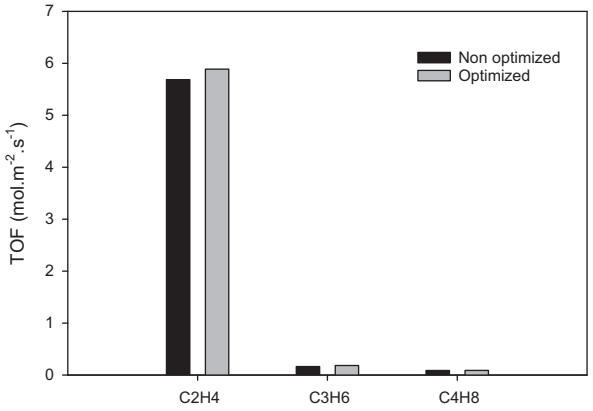

Fig. 8. Turnover frequency for the optimized function.

i.e. more carbon atoms, will tend to increase the production of other carbon related compound such as CO and CO_2. In actual effect, as glycerol initially reacted, the earliest important reactions that may possibly take place are the *glycerol steam reforming reaction* (Eq. (8)) and *decomposition of glycerol* (Eq. (9)). Both reactions are highly reactive and take place spontaneously, with increasing temperature [28]. Hence, it can be assumed that higher glycerol concentration may trigger the inclination toward reactions in Eqs. (8) and (9) to take place strongly. Perhaps subsequent reactions may not at all favor the formation of light olefins with such higher glycerol concentration. Thus, glycerol concentration lower than 30% may be more desirable for the formation of light olefins via methanation reaction route [31]. Hence, in this case, the optimum glycerol concentration should be around 26.9%. Any value more or less than that will reduce the *S* and *Y*, as well as TOF. One plus point for this is that lower glycerol concentration will reduce the cost of the raw material for this process.

$$C_3H_8O_{3(g)} + 3H_2O_{(g)} \leftrightarrow 3CO_{2(g)} + 7H_{2(g)} \quad \Delta H_{298} = 122.89\ \text{kJ/mol} \tag{8}$$

$$C_3H_8O_{3(g)} \leftrightarrow 4H_{2(g)} + 3CO_{(g)} \quad \Delta H_{298} = 246.31\ \text{kJ/mol} \tag{9}$$

3.6. Economic overview

Olefins demand is speculated to rise in future [33]. Since olefin is such an important chemical, various technologies from

Table 5
Multi-objective genetic algorithm optimization using Matlab.

	Temp. (°C)	WHSV (h^{-1})	Glycerol conc. (%)	Optimum (*S*)	Optimum (*Y*)
(a) Predicted (multi-objective genetic algorithm optimization)	650.00	116.54	26.91	22.1	17.8
(b) Observed (experimental)				20.5	16.4
(c) Error				1.54	1.41

Table 7
Comparison of feedstock cost and technologies to obtain olefin.

Technology	Feedstock	Feedstock cost, $ tonne^{-1}	Process	Refs.
Naphtha to olefins	Non renewable, secondary product	600–860 [35]	Cracking, dehydrogenation	[34]
Methanol to olefin (MTO)	Non renewable, secondary product	310–420 [41]	Dehydration, demethanizer, depropanizer, deethanizer, CO_2 removal	[37,38]
Ethanol to olefin (ETO)	Non renewable, secondary product	720–850 [40]	Dehydration	[39]
Methane to olefins	Non renewable, secondary product	395–397 G Joule[c] [43]	Oxidative chlorination	[42]
Coal to olefin (CTO)	Non renewable, primary product	65–300 [46]	Coal to syngas to DME	[45]
Glycerol to olefin (GTO)	Renewable, By product from biodiesel	500–520[a] 130–170[b] [47,48]	Dehydration, dehydrogenation	[18]

[a] Refined.
[b] Crude.
[c] Based on natural gas price in early September 2010 and measured in G Joule.

numerous sources are currently being pursued to produce olefin. Traditionally, olefins are obtained from hydro-cracking of naphtha [34] which is quite expensive due to overpriced raw material costs [35]. There are also other chemical processes used to produce olefins such as elimination reactions, synthesis from carbonyl compounds, olefin metathesis and coupling reactions but all of them still very much depend on petroleum as the main raw material [36]. Table 7 compares feedstock cost and technologies to obtain olefin.

The most widely used process for producing olefins is from methane which proceeds via methanol-to-olefins or Fischer–Tropsch process [37] with synthesis gas as intermediate products. Both processes are capital and energy-intensive [38]. Another process is the ethanol to olefin technology which has already been commercialized by Chematur Engineering Group from Sweden [39]. The process utilizes Syndol based catalysts to react with ethanol to obtain light olefin. Less is known about the actual costing of this process. However, from Table 7, it is noticeable that ethanol price [40] is double the price of methanol [41]. It can be deduced that the utilization of ethanol as feedstock to produce olefin may not be economically attractive. Furthermore, both methanol and ethanol are valuable chemicals, and therefore using it as a feedstock may not be favorable.

Lately, a new way to produce olefins from underutilized methane via a process called oxidative chlorination was developed where methane reacted with hydrogen chloride over lanthanum trichloride ($LaCl_3$) catalyst [42]. Although it is a good process, the fact that methane from natural gas is not renewable undermined the practicality. Nevertheless, the utilization of methane as olefins is a promising option as the feedstock is cleaner and cheaper [43].

Coal-to-olefin (CTO) technology have recently emerged [44]. CTO seems to be the answer to the world olefin supply in the near future since the process is technologically sound [45] and coal price is very cheap [46]. However, the main issue still lies in the fact that coal is non renewable. Hence, there is serious need to explore ways of producing olefins from renewable sources.

The conversion of glycerol produced from biodiesel process to olefin maybe the answer for sustainable olefin supply. Despite the slightly higher refined price [47,48], glycerol has the opportunity to breakthrough as the preferred feedstock due to the development of third generation biofuel that employs algae as a source for producing biodiesel [49]. Lately, Exxon Mobil Corporation declares that they will be testing the commercial viability of algae biofuel as an alternative energy source [50]. The progress of biodiesel production from algae is astounding and can possibly repeat the successful trend of the first generation biofuel. The earlier second generation biofuel as in *Jatropha curcas* [51], waste frying oil [52] and fatty acid distillate [53] has potential to be further developed and cannot be ignored. Both second and third generation biofuel triumphs will ensure continuous glycerol supply.

4. Conclusion

The optimization of catalytic glycerol steam reforming has been investigated. RSM successfully determined the optimum values for each single response. The optimum olefin selectivity, S of 22.9% is achieved at temperature = 737.8 °C, WHSV = 119.4 h^{-1} and glycerol concentration = 28.7%. The optimum response obtained for Y is 17.7% at temperature = 715.9 °C, WHSV = 111.0 h^{-1} and glycerol concentration = 30.1%. Thermodynamic analysis supported the fact that the optimum temperature was established beyond the set range since average optimum temperature formation of light olefin reached its peak at around 700 °C. Multi-objective response genetic algorithm predicted S = 22.1% and Y = 17.8% at the following optimum conditions; temperature = 650 °C, WHSV = 116.54 h^{-1} and glycerol concentration = 26.9% with 2% error between the experimental and predicted values. TOF of the optimized process was higher than the non-optimized, indicating that the optimization effort successfully increase the productivity of the process. Brief economic study revealed that sustainable and cheaper light olefin production can be realized when glycerol is employed as feedstock. It is indeed proven that combination of RSM, multi-objective response and thermodynamic is useful for practical applications to industrial production of glycerol steam reforming. The output of this study can also support the bioenergy industry in managing and generating clean and sustainable energy.

Acknowledgements

The authors would like to acknowledge the following agencies in Malaysia for the financial supports received for this work: Ministry of Higher Education (MOHE) through the project number (Vot 78401) under Fundamental Research Grant Scheme (FRGS), the Ministry of Science, Technology and Innovation (MOSTI) under eScience Fund 03-01-06-SF0963 and Universiti Teknologi Malaysia (UTM).

References

[1] Haas MJ. Improving the economics of biodiesel production through the use of low value lipids as feedstocks: vegetable oil soapstock. Fuel Process Technol 2005;86:1087–96.
[2] Karinen RS, Krause AOI. New biocomponents from glycerol. Appl Catal A: Gen 2006;306:128–33.
[3] Chew TL, Bhatia S. Catalytic processes towards the production of biofuels in a palm oil and oil palm biomass-based biorefinery. Bioresour Technol 2008;99:7911–22.
[4] Huber GW, Corma A. Synergies between bio-and oil refineries for the production of fuels from biomass. Angew Chem Int Ed 2007;46:7184–201.
[5] Pathak K, Reddy KM, Bakhshi NN, Dalai AK. Catalytic conversion of glycerol to value added liquid products. Appl Catal A 2010;372:224–38.
[6] Wolfson A, Dlugy C, Shotland Y. Glycerol as a green solvent for high product yields and selectivities. Environ Chem Lett 2007;5:67–71.

[7] Serafim H, Fonseca IM, Ramos AM, Vital J, Castanheiro JE. Valorization of glycerol into fuel additives over zeolites as catalysts. Chem Eng J 2011;178:291–6.
[8] Corma A, Huber GW, Sauvanaud L, O'Connor P. Biomass to chemicals: catalytic conversion of glycerol/water mixtures into acrolein, reaction network. J Catal 2008;257:163–71.
[9] de Oliveira AS, Vasconcelos SJS, de Sousa JR, de Sousa FF, Filho JM, Oliveira AC. Catalytic conversion of glycerol to acrolein over modified molecular sieves: activity and deactivation studies. Chem Eng J 2011;168:765–74.
[10] Katryniok B, Paul S, Capron M, Dumeignil F. Towards the sustainable production of acrolein by glycerol dehydration. ChemSusChem 2009;2:719–30.
[11] Murata K, Takahara I, Inaba M. Propane formation by aqueous-phase reforming of glycerol over Pt/H-ZSM5 catalysts. React Kinet Catal Lett 2008;93:59–66.
[12] Vasconcelos SJS, Lima CL, Filho JM, Oliveira AC, Barros EB, de Sousa FF, et al. Activity of nanocasted oxides for gas-phase dehydration of glycerol. Chem Eng J 2011;168:656–64.
[13] Hoang TQ, Zhu X, Danuthai T, Lobban LL, Resasco DE, Mallinson RG. Conversion of glycerol to alkyl-aromatics over zeolites. Energy Fuels 2010;24:3804–9.
[14] Adhikari S, Fernando SD, Haryanto A. Hydrogen production from glycerin by steam reforming over nickel catalysts. Renew Energy 2008;33:1097–100.
[15] Adhikari S, Fernando SD, Haryanto A. Hydrogen production from glycerol: an update. Energy Convers Manage 2009;50:2600–4.
[16] Zhou C-H, Beltramini JN, Fan Y-X, Lu GQ. Chemoselective catalytic conversion of glycerol as a biorenewable source to valuable commodity chemicals. Chem Soc Rev 2008;37:527–49.
[17] Pagliaro M, Rossi M. The future of glycerol new usages of a versatile raw material. UK: RSC Green Chemistry Book Series; 2008.
[18] Zakaria ZY, Amin NAS, Linnekoski J. A perspective on catalytic conversion of glycerol to olefins. Biomass Bioenerg
[19] Zakaria ZY, Linnekoski J, Amin NAS. Catalyst screening for conversion of glycerol to light olefins. Chem Eng J 2012;207–208:803–13.
[20] Patcas FC. The methanol-to-olefins conversion over zeolite-coated ceramic foams. J Catal 2005;231:194–200.
[21] Park JW, Kim SJ, Seo M, Kim SY, Sugi Y, Seo G. Product selectivity and catalytic deactivation of MOR zeolites with different acid site densities in methanol-to-olefin (MTO) reactions. Appl Catal A 2008;349:76–85.
[22] Takahara I, Saito M, Inaba M, Murata K. Dehydration of ethanol into ethylene over solid acid catalysts. Catal Lett 2005;105:249–52.
[23] Inaba M, Murata K, Saito M, Takahara I. Ethanol conversion to aromatic hydrocarbons over several zeolite catalysts. React Kinet Catal Lett 2006;88:135–41.
[24] Huang W, Gong F, Fan M, Zhai Q, Hong C, Li Q. Production of light olefins by catalytic conversion of lignocellulosic biomass with HZSM-5 zeolite impregnated with 6 wt.% lanthanum. Bioresour Technol 2012;121:248–55.
[25] Li X, Shen B, Guo Q, Gao J. Effects of large pore zeolite additions in the catalytic pyrolysis catalyst on the light olefins production. Catal Today 2007;125:270–7.
[26] Masih M, Algahtani I, De Mello L. Price dynamics of crude oil and the regional ethylene markets. Energy Econo 2010;32:1435–44.
[27] Wang X, Li S, Wang H, Liu B, Ma X. Thermodynamic analysis of glycerin steam reforming. Energy Fuels 2008;22:4285–91.
[28] Kale GR, Kulkarni BD. Thermodynamic analysis of dry autothermal reforming of glycerol. Fuel Process Technol 2010;91:520–30.
[29] Cornell JA. How to apply response surface methodology. American Society for Quality Control Statistics Division., Winconsin: ASQS.; 1990.
[30] Erbay Z, Icier F. Optimization of hot air drying of olive leaves using response surface methodology. J Food Eng 2009;91:533–41.
[31] Zakaria ZY, Linnekoski J, Amin NAS. Thermodynamic analysis of glycerol to ethylene. International Graduate Conference on Engineering, Science & Humanity 2013, Skudai, Malaysia: Universiti Teknologi Malaysia (UTM); 2013.
[32] Mohammad Fauzi AH, Saidina Amin NA. Optimization of oleic acid esterification catalyzed by ionic liquid for green biodiesel synthesis. Energy Convers Manage 2013;76:818–27.
[33] Zakaria ZY, Amin NAS, Linnekoski J. A perspective on catalytic conversion of glycerol to olefins. Biomass Bioenergy 2013;55:370–85.
[34] Yoshimura Y, Kijima N, Hayakawa T, Murataa K, Suzuki K, Mizukami F, et al. Catalytic cracking of naphtha to light olefins. Catal Surv Jpn 2000;4:157–67.
[35] Dillon T, London RY. Crude oil falls help to push spot naphtha lower. ICIS Chemical Business; 2010. p. 24.
[36] Ren T, Patel M, Blok K. Olefins from conventional and heavy feedstocks: energy use in steam cracking and alternative processes. Energy 2006;31:425–51.
[37] UOP. UOP/HYDRO MTO process -– Methanol to olefins conversion. Process Technology and Equipment; 2004.
[38] Soundararajan S, Dalai AK, Berruti F. Modeling of methanol to olefins (MTO) process in a circulating fluidized bed reactor. Fuel 2001;80:1187–97.
[39] Chematur EEG. Business area biomass chemicals – ethylene from ethanol. Chematur Engineering AB; 2010.
[40] ICIS. Ethanol prices and pricing information. In: R.B.I. Limited, (Ed.); 2011.
[41] Methanex. Methanol price. Methanex Corporation ;2012.
[42] Reisch M. Dow issues methane challenge – call for proposals targets direct conversion of methane into feedstocks. Chem Eng News 2007;85:12.
[43] Global K. Natural gas prices set for gains. The street; 2010. <http://www.thestreet.com/story/10851133/1/natural-gas-prices-set-for-gains.html> [accessed 29.01.14.].
[44] Burridge E. Looming excess methanol could marginalize China production. ICIS Chemical Business; 2010. p. 17.
[45] Plotkin JS, Coleman HJ. PERP program – cole to olefins. Nexant Chem System; 2007.
[46] Maher K. Chinese slowdown idles U.S. Coal Mines; 2012. Available from: <http://online.wsj.com/article/SB10000872396390443890304578010472748244256.html>. 2012 [accessed 29.01.14.]
[47] Seng S. Asia glycerine prices poised to rise on tight supply in Q1 ICIS news; 2010.
[48] ICIS. ICIS Pricing – 2nd May 2012 – Glycerine (US Gulf); 2012.
[49] Doan TTY, Sivaloganathan B, Obbard JP. Screening of marine microalgae for biodiesel feedstock. Biomass Bioenergy 2011;35:2534–44.
[50] Tan J, Seng LP. Exxon explores algae biofuels as alternative energy. Kuala Lumpur: Reuters; 2010.
[51] Kumar Tiwari A, Kumar A, Raheman H. Biodiesel production from jatropha oil (*Jatropha curcas*) with high free fatty acids: An optimized process. Biomass Bioenergy 2007;31:569–75.
[52] Zheng S, Kates M, Dubé MA, McLean DD. Acid-catalyzed production of biodiesel from waste frying oil. Biomass Bioenergy 2006;30:267–72.
[53] Chongkhong S, Tongurai C, Chetpattananondh P, Bunyakan C. Biodiesel production by esterification of palm fatty acid distillate. Biomass Bioenergy 2007;31:563–8.